Calibration of Electric Coaxial Near-Field Probes and Applications

Yingjie Gao, Andreas Lauer, Qiming Ren, and Ingo Wolff, *Fellow, IEEE*

***Abstract*—A new calibration technique for application to near-field probes has been developed. For this, a simple electric coaxial near-field probe for application in the 0.05–20-GHz band has been developed, theoretically analyzed, and calibrated using a known field. By using the finite-difference time-domain (FDTD) method, this field probe is theoretically analyzed to determine its most sensitive probe segment. Taking the amplitude of the normal electric field at this segment as a known field, the probe is calibrated by defining a performance factor (PF), which is the ratio of the known field amplitude to the probe signal amplitude. Comparing the calculated results with measured results, the agreement is good. Additionally, the measurements are experimentally characterized with respect to the influence of the distance between the probe and the device-under-test (DUT), the influence of the input signal on the probe, and the spatial resolution. Two measurement examples are demonstrated, which investigate the mode and field distribution within passive coplanar microwave components.**

***Index Terms*—Electric-field probes, measurement techniques.**

I. Introduction

IN THE LAST years, great progress has been made in the development of microwave elements and circuits. The development of complex circuits and systems requests new test systems in microwave design. The measurement of only input and output signals using a network analyzer (NWA) is not sufficient to analyze the performance and errors because, in many cases, the information obtained is not sufficient to localize the cause of the errors. A nonconducting scanning microwave-field probing technique has been developed, which measures the surface electric- and magnetic-field distributions of the circuits. This technique can be used for performance and failure analysis in microwave circuits. An electrooptical probing system, which is normally applicable for GaAs substrates, provides a very wide bandwidth and a good resolution [1]. A scanning-force microscope-based test system can be used for a device internal electrical characterization of monolithic microwave integrated circuits (MMIC's) [2]. A modulated scattering imaging system, using electric monopoles and dipoles, can be used to simultaneously detect normal and tangential electric-field intensities and the net electrical phase delay within a microwave circuit [3]. An electric monopole probe has been applied to investigate the electric-field normal component distribution of microwave circuits [4], [5]. Some miniaturized magnetic-field probes have been reported for measurements in high-frequency planar circuits [6], [7].

Manuscript received November 25, 1997; revised July 17, 1998. The work of Q. Ren was supported by the German Academic Exchange Service (DAAD).

Y. Gao and A. Lauer are with the Institute of Mobile and Satellite Communication Techniques (IMST), Kamp-Lintfort 47475, Germany.

Q. Ren and I. Wolff are with the Department of Electrical Engineering, Gerhard Mercator University Duisburg, D-47057 Duisburg, Germany.

Publisher Item Identifier S 0018-9480(98)08002-8.

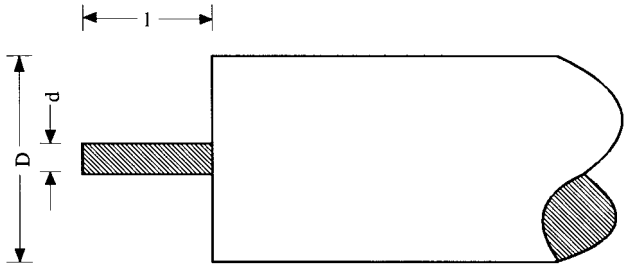

Fig. 1. Coaxial electric-field probe.

This paper reports on a measurement system setup, probe characterization (including a theoretical analysis of the probe, probe calibration, the change of the output signal with the distance between the probe and the device-under-test (DUT), and the spatial resolution of the probe), investigation of passive coplanar microwave circuits, and error analysis.

II. Probe Characterization

The electric near-field probe for z-coordinate (EPZ) for measuring the normal electric-field component in z-direction is very simply constructed from a 50-Ω semirigid coaxial cable. Two such electric-field probes are discussed in this paper. The geometry of the probe is shown in Fig. 1. Probe EPZ1 has an outer diameter D of 508 μm and an inner conductor diameter d of 112 μm, extending 300 μm beyond the outer conducting shield. Probe EPZ2 has an outer diameter D of 1190 μm and an inner conductor diameter d of 287 μm, extending 1000 μm beyond the outer conducting shield.

A. Theoretical Analysis of the Probe

The coaxial probe under consideration can be simulated using, e.g., the well-known finite-difference time-domain (FDTD) method [8]–[9]. A two-dimensional (2-D) FDTD derivation in cylindrical coordinates is used here to generate a simple, but accurate, model of the probe.

Fig. 2 shows the arrangement used for the FDTD simulation including perfectly matched layer (PML) boundary conditions [10], [11]. The probe is looked at as a special kind of antenna

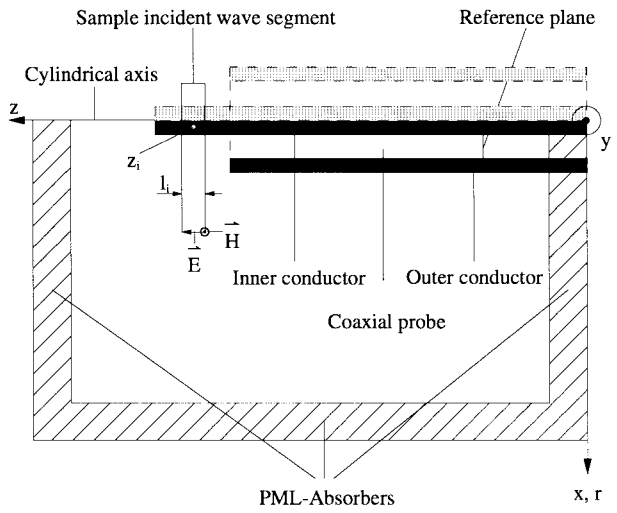

Fig. 2. Arrangement for FDTD simulation of the coaxial probe.

excited by a primary electromagnetic field $F_p(x,y,z,t)$, which would be the exact field in the absence of the probe, and which is identical to the incident plane wave. A secondary field $F_s(x,y,z,t)$ is generated by the probe, in a way such that the sum $F(x,y,z,t) = F_p + F_s$: 1) obeys Maxwell's equations because F_p and F_s are appropriate field-solutions and 2) fulfills the boundary conditions on the probe surface.

The FDTD simulations, therefore, are performed for the secondary field only, using the negative primary tangential electric field on the metallic surfaces as an excitation. For generating a simple model, the primary field is chosen to be a plane wave propagating in x-direction, polarized to have E_z and H_y field components only (see Fig. 2). The electric-field component E_z is chosen to be an arbitrary excitation field $E_{z,0}(t)$ independent of z on the z-axis. The wave excites only a segment $z \in s_i = [z_i - l_i/2, z_i + l_i/2]$ (see Fig. 2) of the probe, the z_i's are the locations of the center points of the segments, and the l_i's are their lengths. The results are the voltage amplitudes $V_{i,0}(t)$ of the wave excited in the coaxial line. The ratio $A_{i,0}(\omega) = V_{i,0}(\omega)/E_{z,0}(\omega)$ is defined in the frequency domain. A couple of simulations with different wave segments s_i are used to obtain a complete profile of the probe sensitivity, i.e., the value of the voltage excited in the coaxial probe with respect to the electric field in the segment on the z-axis.

The probe output for an arbitrary primary field F_p can then approximately be written in the frequency domain as

$$V(\omega) \approx \sum_{i=1}^{N} E_{p,z}(x=0, y=0, z=z_i, \omega) A_{i,0}(\omega) \quad (1)$$

using just the z-components of the primary electric field at several points on the z-axis as input data. From the results of the FDTD simulation for frequencies below 20 GHz, the factor $A_{i,0}(\omega)$ can be written as

$$A_{i,0}(\omega) = B_{i,0}\omega \quad (2)$$

i.e., $A_{i,0}(\omega)$ is linearly dependent on the frequency ω.

Using a factor $C_{i,0}$, which is written as

$$C_{i,0} = B_{i,0} E_i / l_1 \quad (3)$$

where E_i is the intensity of a typical normal electric field of the microstrip line at the segment z_i, the most relevant segment of the probe can be determined. From the results of the simulation, the segment of the probe is most relevant at $z_i = 300$ μm. Using the intensity of the normal electric field of the microstrip line in this position, the probes can be calibrated.

B. Probe Calibration

The calibration method compares the measured electric field and the calculated electric field over a microstrip transmission line. By comparing the amplitude of the probe signal from measurement and the amplitude of the normal electric field from a standard static finite-difference simulation over the same region above the transmission line, the ratio of the measured signal amplitude and calculated field amplitude can be determined.

A microstrip transmission line is used for probe calibration. This transmission line is fabricated on a ceramic substrate with dielectric constant of 9.8 and a substrate height of 635 μm. The width of the transmission line is 700 μm. For the calibration, the transmission line is terminated by a 50-Ω resistive load, and the probe is set at a height of 50 μm above the substrate.

For the smaller probe EPZ1, there is no standard subminiaturized class-A (SMA) connector available, so a slightly larger SMA connector is used in this case. Therefore, the performance of this probe is not so good, and some resonant frequencies may be recognized in Fig. 3. These resonant frequencies influence the signal measurement of the probe over frequency. The calibration frequencies are chosen in such a way that the reflection coefficient of the probe has a local minimum or maximum at these frequencies. The absolute input power, probe signal, and connector loss from coaxial cable to microstrip line are measured using a spectrum analyzer for this frequencies. After calculation with these parameters, the absolute probe signal can be obtained with a constant input power of -10 dBm directly on the transmission line. Using this -10-dBm input power to excite the microstrip transmission line, the magnitude of the normal electric field at a height of 350 μm for the probe EZP1 and 1050 μm for the probe EPZ2 above the substrate can be calculated using the FDTD program. The FDTD simulation proves that at these heights, the probes EPZ1 and EPZ2 have the high sensitivities of the normal electric field of the microstrip line, respectively. A performance factor (PF) (with dimension $1/m$) is defined as the ratio of the amplitude of the normal electric-field value at the position of the probe to the amplitude of the actual measured voltage [12].

The PF of the probe EPZ1, which is derived as a function of frequency, is shown in Fig. 3(a). Using the fitting curve of the PF as a calibration curve, the error is ± 7 dB because the reflection coefficients are not constant in this frequency range. For a more accurate measurement, a calibration data table must be used.

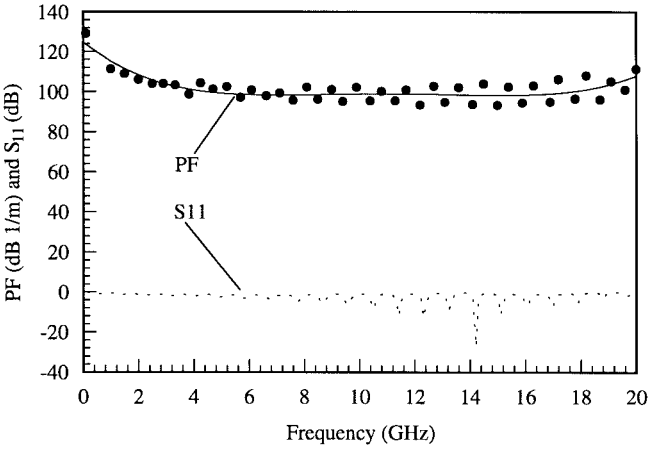

(a)

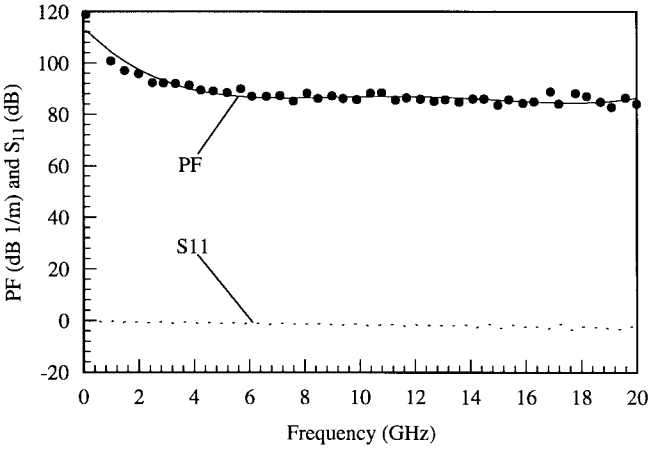

(b)

Fig. 3. The PF and reflection coefficients S_{11} of the coaxial electric-field probe. (a) EPZ1. (b) EPZ2.

For the larger probe EPZ2, the amplitude of the reflection coefficient changes very little over the frequency range from 100 MHz to 20 GHz, as shown in Fig. 3(b). Thus, the fitting curve of the PF can be used as a calibration curve at frequencies below 17 GHz. The error then will be ± 3 dB. Above 17 GHz, the performance of the two probes is poor probably because SMA connectors are used. The performance of the probe should be better if a K connector is used.

Fig. 4 shows the measured and calculated normal electric-field distribution over a cross section of a microstrip line at 11.8 GHz. The measurement is taken using a spectrum analyzer, which measures the absolute probe signal. This measured signal is multiplied by the PF at the frequency of 11.8 GHz. The result determined in this way is shown in Fig. 4. It can be seen that the agreement between the measured and calculated results is good near the conductor, but the measured probe signal is larger than the calculated results above the substrate area. This is due to the electric field above the substrate being much smaller than above the conductor. In these positions where the normal electric-field components are smaller, the measurement errors are bigger. Using the PF, a quantitative value of the field distribution in microwave circuits can also be measured in these cases.

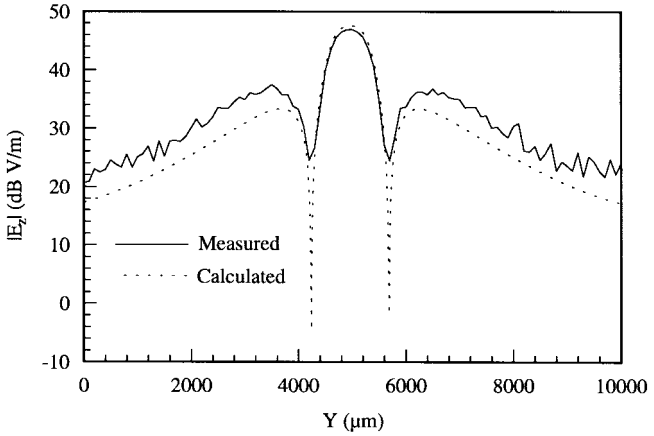

Fig. 4. Comparison between the measured and calculated normal electric field at a cross section of the microstrip line at 11.8 GHz. Substrate: Al_2O_3, $\varepsilon_r = 9.8$, $h = 635$ μm, $w = 700$ μm.

The absolute-value measurement is especially important for electromagnetic compatibility (EMC) applications where the intensity of the field in electronic circuits and instruments is a significant criterion.

C. Change of the Probe Signal with the Distance from the Substrate and with the Input Power

A microstrip line terminated with a coaxial 50-Ω load is used as DUT for characterizing the probe. This microstrip line is constructed on an RT-Duroid substrate with a dielectric constant $\varepsilon_r = 2.3$ and a substrate thickness of $h = 790$ μm. Firstly, the probe signal changing with the distance between the probe and the DUT is tested. For this purpose, the microstrip transmission line is excited with 10-dBm input power at 1 GHz. The probe signal is measured using a spectrum analyzer. The measured magnitude of the probe signal is shown in Fig. 5(a). For this measurement, the probe signal was changed by about 8.5 dB (if the probe height above the substrate was varied from 20 to 320 μm). The probe signal decreases rapidly with the distance when the probe is near the DUT, e.g., in a distance of 100 μm. The dependence of the probe signal on the input power of the microstrip line at 1 GHz is shown in Fig. 5(b). Since the electric-field probe is passive, the probe signal is linearly proportional to the input power of the microstrip line. The maximum error is about 0.3 dB. The sensitivity of the measurement system is also tested by measuring the change of the probe signal with the variation of the input power. The sensitivity of the near-field measurement system is below 0.5 dBm.

D. Spatial Resolution

In order to test the spatial resolution of the probe, a five-finger interdigital capacitor has been fabricated, as shown in Fig. 6. It is fabricated on a ceramic substrate ($\varepsilon_r = 9.8$, $h = 635$ μm). The finger widths and gapwidths are both 100 μm. The vertical electric-field distribution of the interdigital structure at 7.0 GHz, which is measured with the electric probe, is shown in Fig. 7. For the measurements shown below, a vector NWA is used as a transmitter and receiver. From the

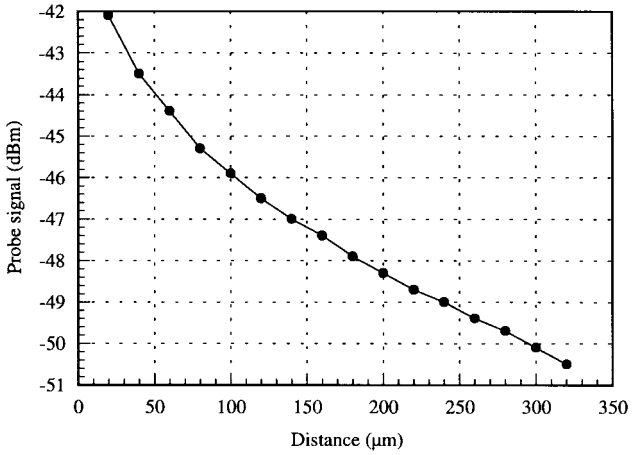

(a)

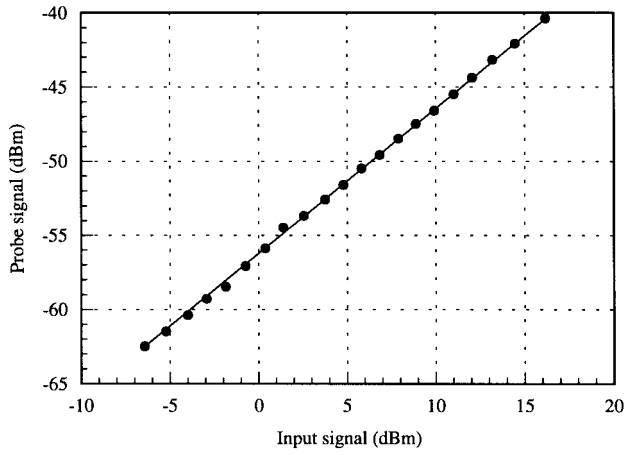

(b)

Fig. 5. (a) The probe signal changes with the distance between the probe and the DUT. (b) The probe signal changes with the input signal of the microstrip line at 1 GHz.

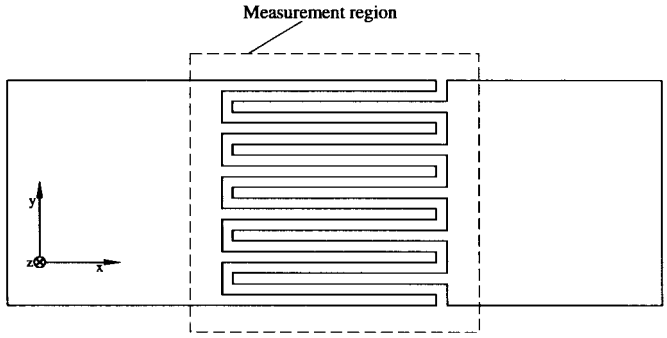

Fig. 6. The layout of a five-finger interdigital capacitor. Substrate: Al_2O_3, $\varepsilon_r = 9.8$, $h = 635\ \mu$m, $w = 100\ \mu$m, $s = 100\ \mu$m.

experimental results, it can be seen that a spatial resolution of the field probe smaller than 100 μm can be reached.

III. Applications

A. Investigation of Near-Field Distributions of Coplanar Microwave Circuits

1) Coplanar Waveguide (CPW) Transmission Line: Traditionally, microstrip lines have been widely used as the primary transmission line for hybrid and monolithic microwave and millimeter integrated circuits. However, during the last years, there has been considerable interest in CPW's for application in microwave integrated circuits (MIC's) and especially in MMIC's due to their attractive features. Since for such a structure the signal line and ground planes are all placed on one side of the substrate, active and passive devices can be mounted both in shunt and series connection, eliminating

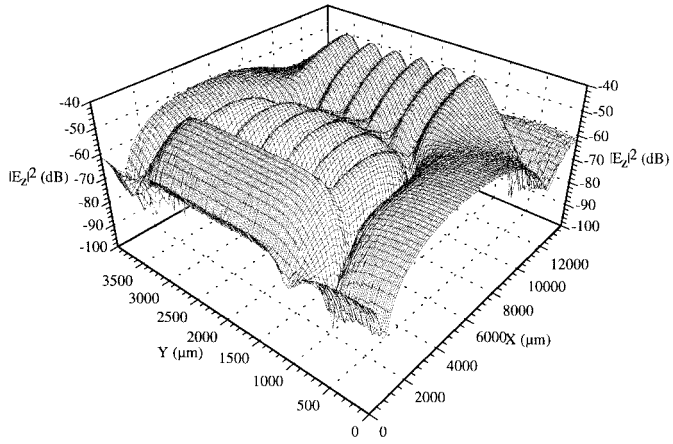

(a)

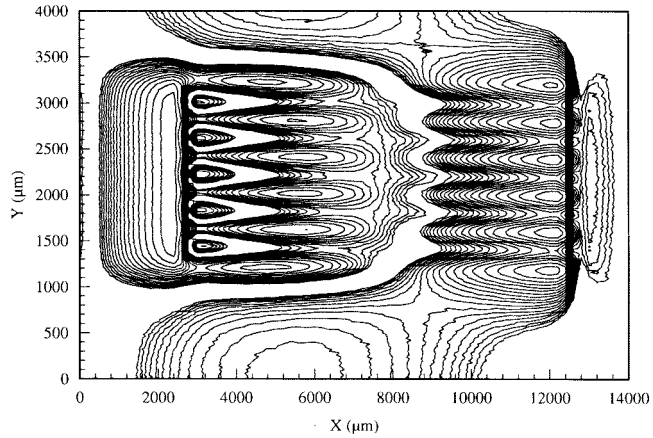

(b)

Fig. 7. Measured $|E_z|^2$ for a five-finger interdigital capacitor at 7.0 GHz.

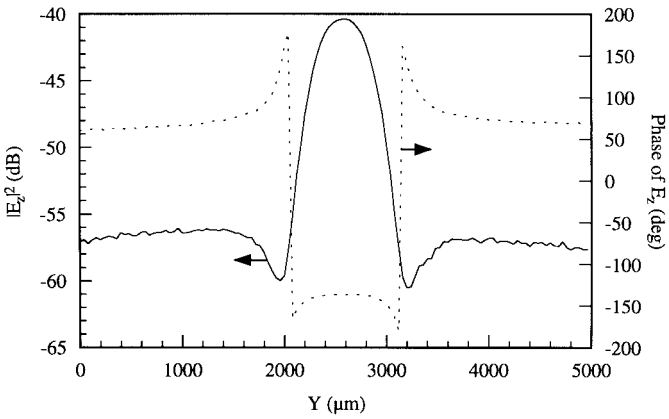

Fig. 8. Magnitude and phase distribution of the normal electric field at a across section of a CPW transmission line.

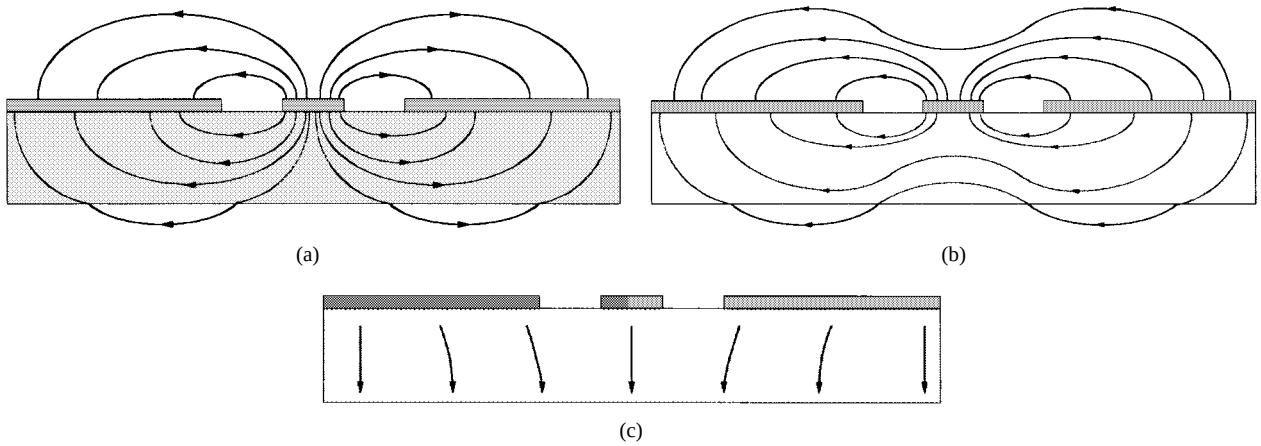

Fig. 9. Electric-field distribution of a coplanar transmission line. (a) Coplanar mode (even mode). (b) Slot-line mode (odd mode). (c) Microstrip-line mode.

the need for via holes and reducing the associated parasitic inductance [13]. In contrast to the microstrip line, for which the characteristic impedance depends on the thickness of the substrate, the characteristic impedance of a coplanar transmission line is mainly determined by the relation of w/d, where $d = w + 2s$ with w the line width and s the gapwidth. For values $h < d$, the thickness h of the substrate has some influence on the characteristic impedance, but for $h > d$, this influence may be neglected. Such an independence of the characteristic impedance from the thickness of the substrate makes it possible to realize transmission lines with equal impedance, but with lines of different w- and s-values. This gives a great flexibility in the design of microwave circuits.

A CPW transmission line has been fabricated and tested. It is constructed on a ceramic substrate with $\varepsilon_r = 9.8$ and with a thickness of 635 μm. The center conductor width is 500 μm and the slot width is 217 μm. Fig. 8 shows the amplitude and phase of the normal electric-field distribution of the CPW transmission line terminated with a 50-Ω load measured at a height of 50 μm above the substrate. As expected from electrostatic theory, the normal electric-field peak is at the center conductor and the minimum values are across the slot, the phase of the normal electric field has about 1800 difference between the center conductor and ground plane.

2) Coplanar T-Junction for Mode Investigation: Compared to the conventional microstrip design, the CPW, which works in the fundamental coplanar mode (even mode) as shown in Fig. 9(a), has several advantages as mentioned above. However, the main obstacle facing CPW is the excitation of the parasitic (odd) slot-line mode in nonsymmetric CPW circuits, as shown in Fig. 9(b). The excitation of the odd mode is essential in structures like T-junctions due to different propagation times along the corresponding slots. The parasitic mode disturbs the wanted field distribution and tends to radiate. It, therefore, must be eliminated or reduced. The conventional method of eliminating the parasitic slot-line mode is to use air-bridges [14]. In practical applications of CPW's, the substrate often is mounted directly on a metallic ground plane to avoid a fracture of the fragile substrate. Under these conditions, a microstrip-like (MSL) mode can be excited on a CPW of finite-width ground planes, as shown in Fig. 9(c). Jackson identified this mode as a coplanar microstrip mode for a CPW with conductor backing [13]. Shigesawa and Tsuji called it a CPW surface-wave-like (SWL) mode [15]. In this mode, all three conductors are on the same potential. Theoretical studies of asymmetric CPW discontinuities are presented in [16] and [17]. They determine the s-parameters at the ports. The electrooptic sampling technique has been used to investigate coplanar microwave waveguide in [18] and [19]. This technique delivers detailed information about the mode transformations at the discontinuities.

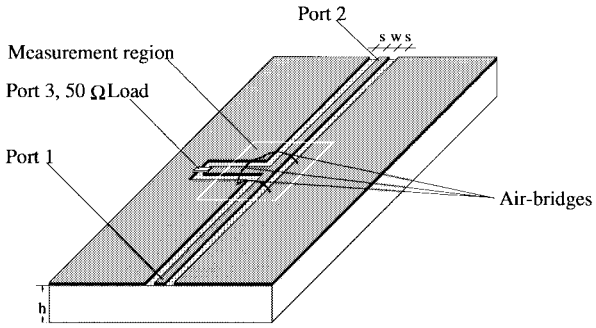

Fig. 10. Construction of a coplanar T-junction with air-bridge.

To analyze the function of the air-bridges in coplanar microwave circuits, a T-junction with different numbers of air-bridges is fabricated, as shown in Fig. 10. This coplanar T-junction has a conductor width of 500 μm and a gapwidth of 217 μm. It is fabricated on ceramic substrate with a dielectric constant of 9.8 and a thickness of 635 μm. Port 3 is terminated with a 50-Ω impedance and port 2 is terminated with a 50-Ω coaxial load.

The normal electric-field distribution of the T-junction without air-bridges has been measured with the probe EPZ, as is shown in Fig. 11. This measurement is taken in a region of 10 000 $\times$ 10 000 μm at a height of 100 μm above the substrate. The measurement steps are 100 μm in x- and y-directions, respectively. In order to analyze the measured results in detail, the field distribution in three cross sections are selected and shown in Fig. 12. The transmission line at port 1 transports a nearly pure coplanar mode (even mode), as shown in Fig. 12(a). The reflected signal is small. In this section, the

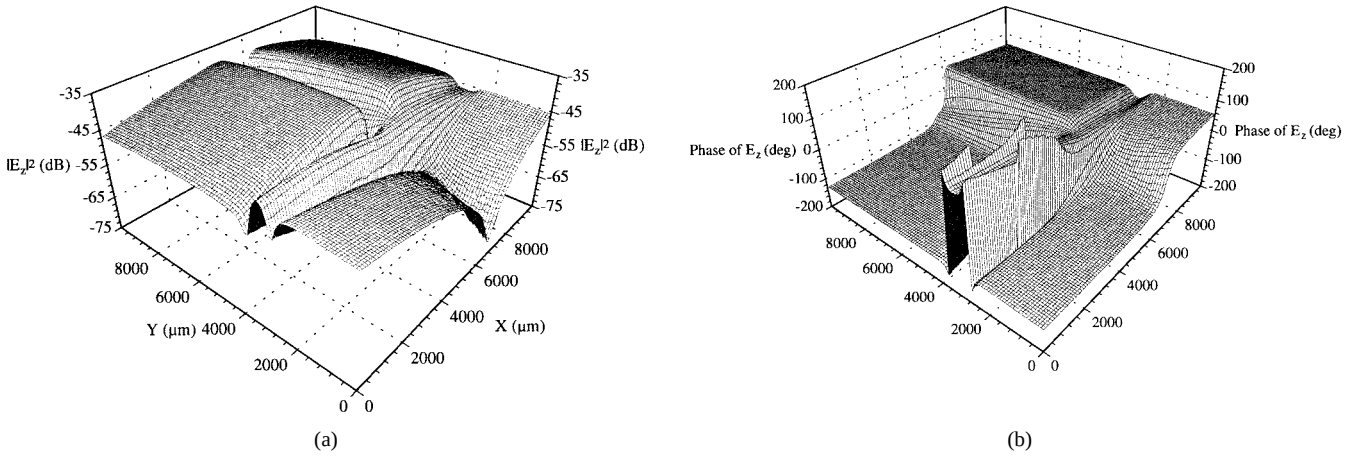

Fig. 11. Normal electric-field distribution of a coplanar T-junction without air-bridge. (a) Magnitude $|E_z|^2$. (b) Phase of E_z.

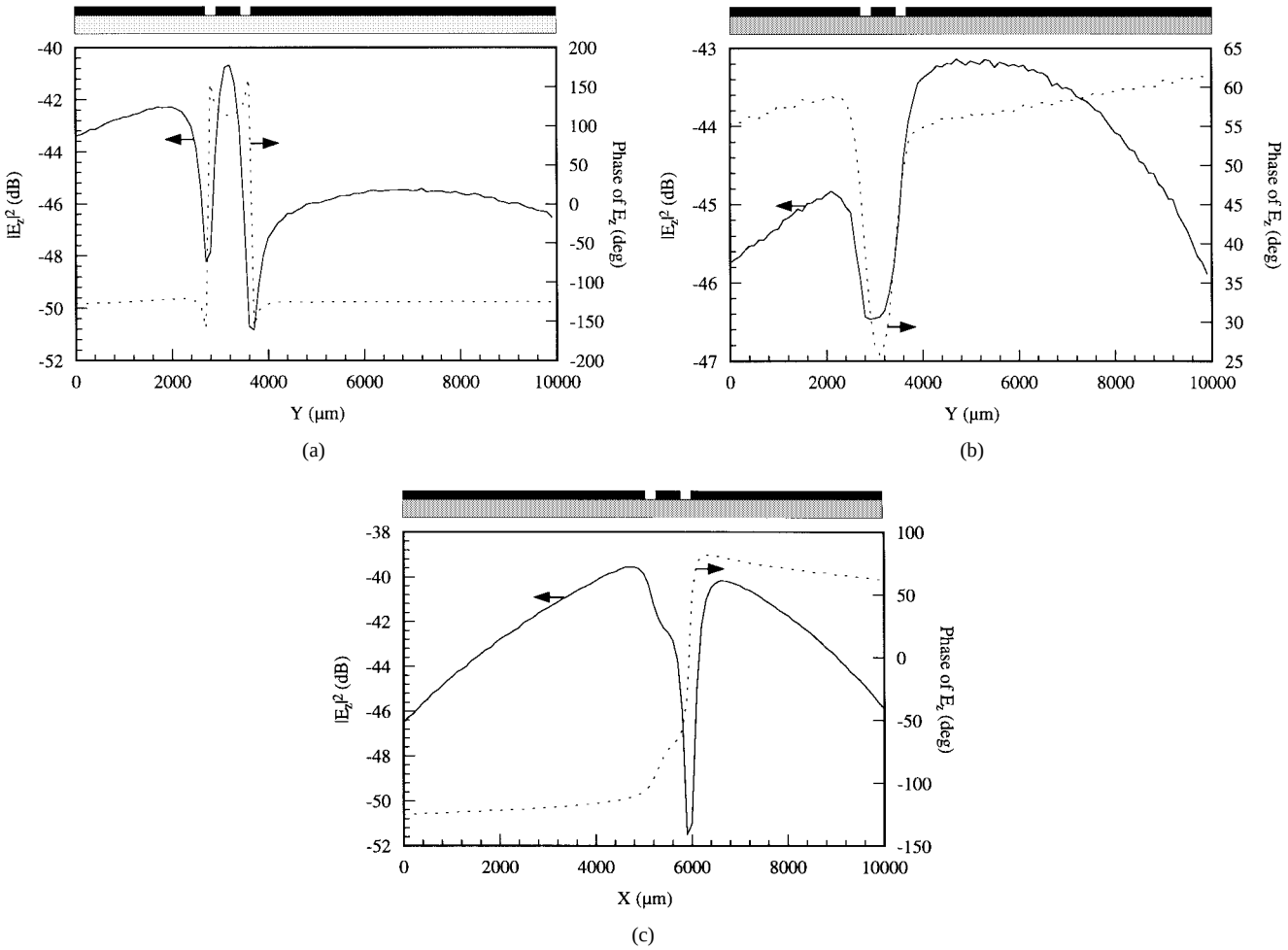

Fig. 12. Normal electric-field distribution of T-junction without air-bridge at sections (a) $x = 0$, (b) $x = 10\,000\ \mu$m, and (c) $y = 10\,000\ \mu$m.

maximum normal electric field is in the middle of the center conductor, and the minimum normal electric fields are near the slots. The phases of the normal electric fields have about 1200 difference between the center conductor and ground planes. Near port 2, the amplitude and the phase of the electric field are almost constant, as shown in Fig. 12(b) (consider the given scaling in this figure). This is the typical microstrip mode or SWL-mode distribution. Due to the discontinuity of the T-junction, such a microstrip mode can be excited, especially in a circuit without air-bridges [20]. Near port 3, the minimum normal electric field is measured in one slot between the center conductor and the ground plane, as shown in Fig. 12(c). In the second slot, the field is on a maximum value. This field distribution is typical for a superposition of an even and odd mode on the CPW. The phase difference between the center conductor and ground plane across the first slot is about to

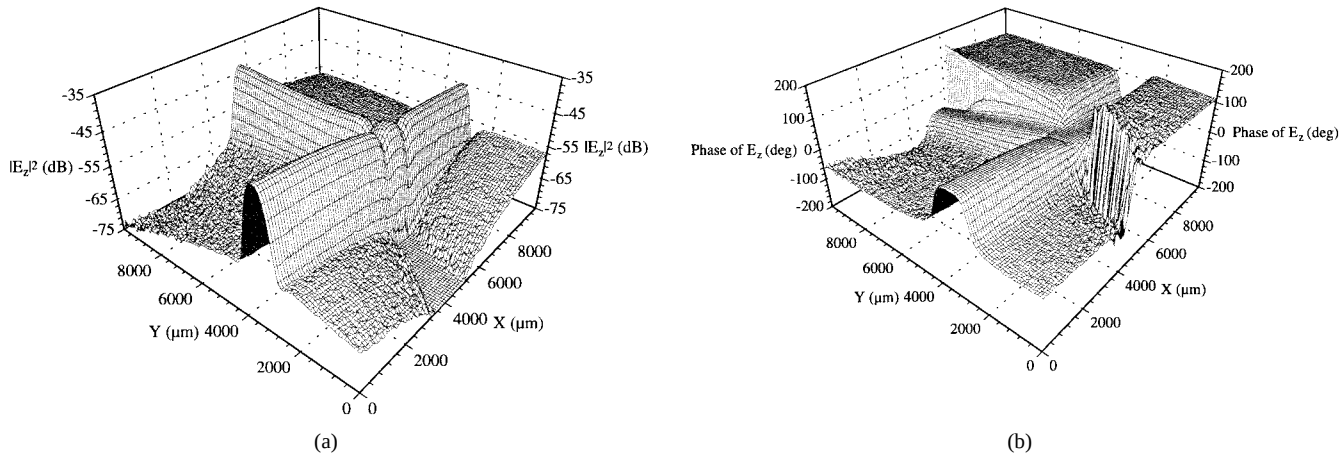

Fig. 13. Normal electric-field distribution of a coplanar T-junction with air-bridges. (a) Magnitude $|E_z|^2$. (b) Phase of E_z.

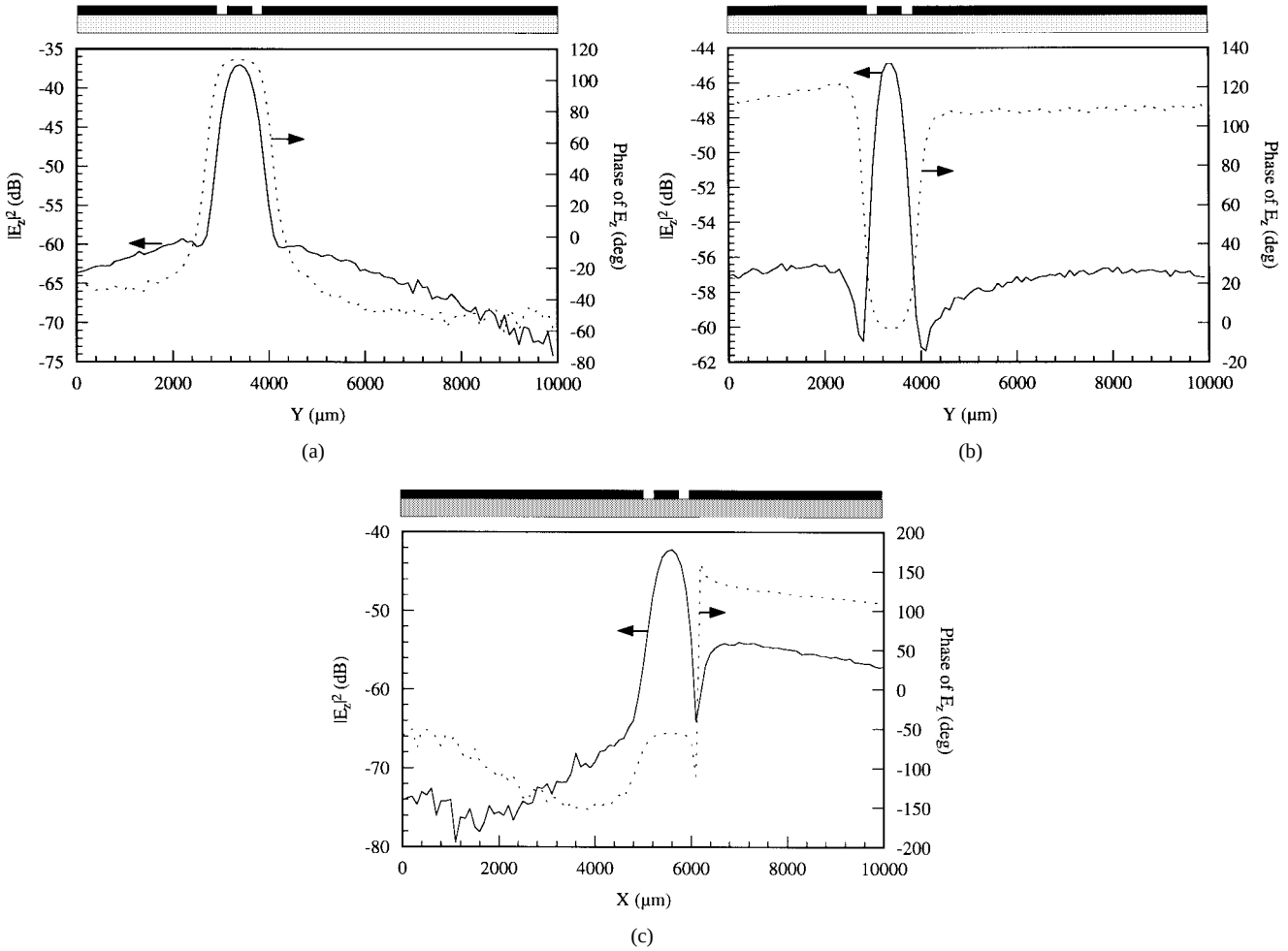

Fig. 14. Normal electric-field distribution of T-junction with air-bridges at sections (a) $x = 0$, (b) $x = 10\,000$ μm, and (c) $y = 10\,000$ μm.

1600. There is only a little phase difference of about 400 between the center conductor and ground plane across the other slot.

Fig. 13 shows the normal electric-field distribution of the T-junction with three air-bridges, as shown in Fig. 10. The normal electric-field distributions at three different cross sections are shown in Fig. 14. From this figure, it can be seen that at all three ports the transmission modes are of coplanar mode, even though it is not a pure even mode at port 3. The magnitude of the normal electric field is about 25 dB and has a 13-dB difference between the center conductor and ground plane near ports 1 and 2, respectively, as shown in Fig. 14(a) and (b). The field distributions are also highly symmetric at port 2. The phase differences between the center conductor and the ground planes are about 180° and 110° at ports 1 and 2, respectively. However, at port 3, due to the discontinuity,

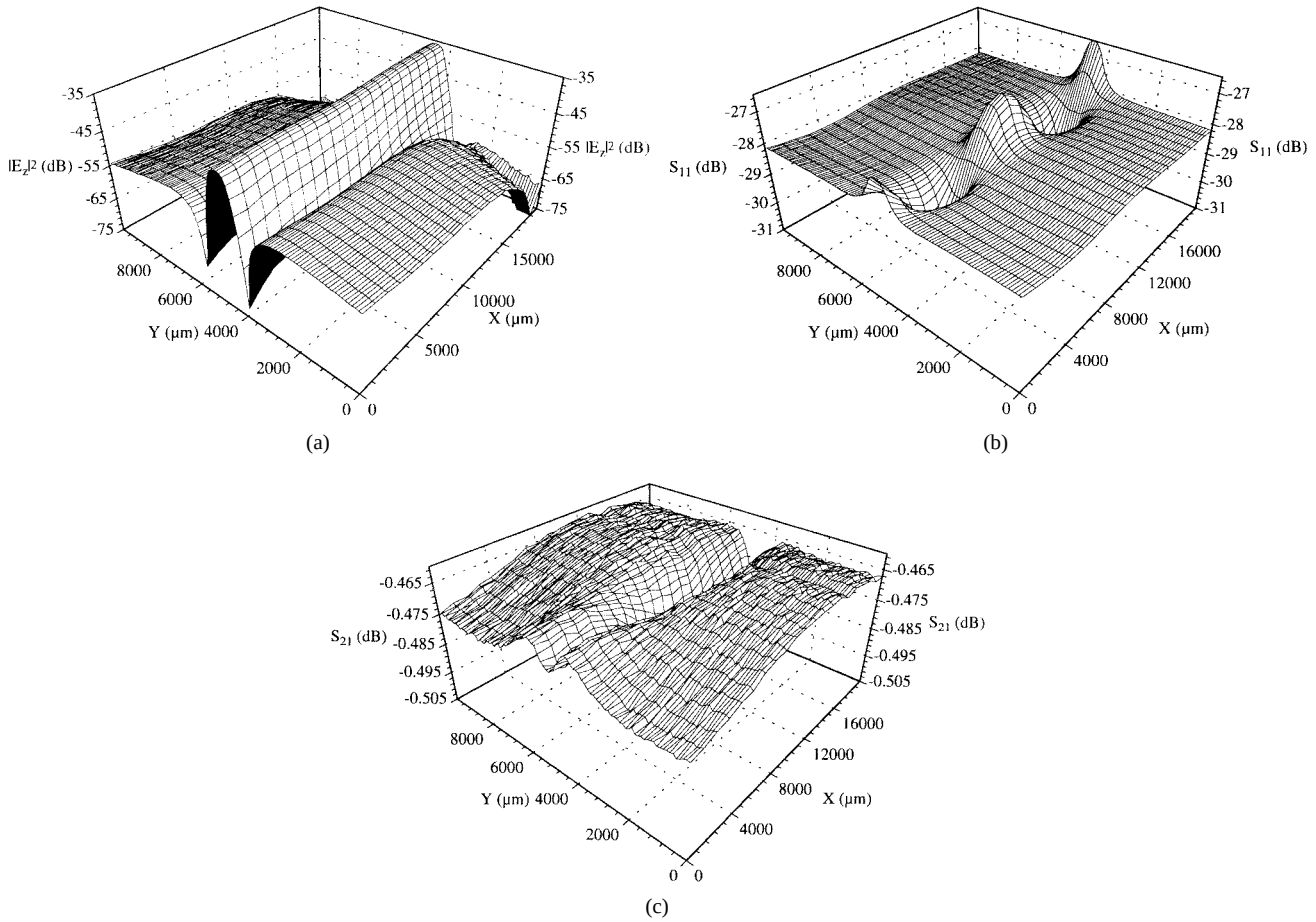

Fig. 15. The investigation of the influence of the probe on the microstrip line. (a) The normal electric field distribution. (b) Reflection coefficient S_{11}. (c) Transmission coefficient S_{21}.

the field distribution is not very symmetrical, as shown in Fig. 14(c). There is a phase difference of about 100° between the center conductor and ground planes.

From these measurements at a T-junction with and without air-bridges, it can be seen that the near-field measurement system can give very detailed information about the transmission modes in coplanar and other microwave circuits. It is a very helpful tool for the design of microwave circuits.

IV. Error Analysis

The measurement principle of the electric and magnetic near-field probes is to couple the electromagnetic near field of the DUT to the probes. Therefore, the probes must be positioned near the DUT. Since the probe consists of metal and dielectric material, the probes certainly influence the DUT. If the probe is set in a proper position to the DUT, the influence can be so small that it may be neglected.

To estimate the coupling effect between the probes and the DUT, the change of the scattering parameters S_{11} and S_{21} of the DUT (measured with an NWA) when the probe enters the field can be observed. It is very difficult to give an absolute value of the probe influence on the DUT because this kind of influence depends not only on the field probe, but also on the DUT, e.g., the substrate of the DUT, frequency, and fabrication technology (microstrip or coplanar technology).

A microstrip line is used to estimate the influence of the probe on the DUT. The microstrip line with a strip width of 700 μm is fabricated on a ceramic substrate with a dielectric constant of 9.8 and height of 635 μm. First, the normal electric-field distribution at a height of 50 μm above the microstrip line and the reflection coefficient S_{11} at port 1 of the microstrip line and at a frequency of 5 GHz are measured (the line is terminated by a 50-Ω load) using the coaxial electric-field probe EPZ1. The results are shown in Fig. 15(a) and (b). Then port 2 of the NWA is connected to port 2 of the microstrip line, the transmission coefficients of the microstrip line at 5 GHz are measured during the movement of the field probe perpendicular to the line direction at a height of 50 μm above the microstrip line, as shown in Fig. 15(c). Without the field probe above the DUT, the scattering parameters S_{11} and S_{21} of the microstrip line should be the original values of the undisturbed structure. After setting the field probe above the microstrip line, the scattering parameters change. This change of the scattering parameters may be defined as the disturbance error of the field probe.

From Fig. 15(a), it can be seen that at a height of 50 μm above the microstrip line, the probe may deliver a strong enough signal to give detailed information of the normal electric-field distribution. In this position, the probe signal has a dynamic range of about 40 dB. Since the microstrip line is terminated by a 50-Ω load, the reflection coefficient S_{11} is very

small, about −28.0 dB, and the transmission coefficient S_{21} is large, about −0.47 dB. These values represent an extreme situation in microwave circuits. For the very small value of S_{11}, the change of the reflection coefficient is about ±3 dB, as shown in Fig. 15(b). It can also be seen that the changes of S_{11} are not constant for different positions of the probe above the middle of the conductor. If Fig. 15(b) is compared to Fig. 15(a), it may be recognized that because of the small value of the S_{11} parameter, the change of the reflection coefficient when moving the probe may not be detected in the probe signal [see Fig. 15(a)]. Nevertheless, Fig. 15(b) also shows the standing wave, which is still available on the matched line even if it has a very small amplitude. This phenomenon cannot be recognized in the probe signal. Since the transmission coefficient S_{21} is very large, as shown in Fig. 15(c), the influence of the probe on this value is very small, about 0.05 dB. If the field probe is placed higher than 50 μm above the DUT, the influence of the probe is smaller. From these measurements, it can be seen that the disturbances of the near-field probe on the DUT are so small that in most cases they can be neglected.

V. Conclusions

In order to measure the electric field inside microwave circuits in a quantitative manner, a simple coaxial electric-field probe is developed, which is based on a known electric-field distribution of a microstrip line. Multiplying the measured probe signal with a defined PF, an absolute intensity of the electric field can be determined. Comparing the measured and the calculated results, the agreement is found to be good. Coplanar microwave circuits have been investigated using the calibrated electric-field probe. From the measurement results, it can be seen that the field probe is very useful for the analysis of field and modes in coplanar circuits. Other applications demonstrate that the measurement technique can be used to measure the scattering parameters of microwave circuits at an arbitrary position inside the structures.

References

[1] G. David, S. Redlich, W. Mertin, R. M. Bertenburg, S. Koßlowski, F. J. Tegude, E. Kubalek, and D. Jäger, "Two-dimensional direct electro-optic field mapping in a monolithic integrated GaAs amplifier," in *Proc. 23rd European Microwave Conf.*, Madrid, Spain, Sept. 1993, pp. 497–499.

[2] C. Böhm, M. Otterbeck, S. Lipp, R. Reuter, A. Leyk, W. Mertin, F. J. Tegude, and E. Kubalek, "Design and characterization of integrated probes for millimeter wave applications in scanning force microscopy," in *IEEE MTT-S Int. Microwave Symp. Dig.*, vol. 3, San Francisco, CA, June 18–20, 1996, pp. 1529–1532.

[3] T. P. Budka, S. D. Waclawik, and G. M. Rebeiz, "Near electric field mapping above X-band MMIC's using modulated scattering," in *IEEE MTT-S Int. Microwave Symp. Dig.*, vol. 3, San Francisco, CA, June 18–20, 1996, pp. 1703-1706.

[4] J. S. Dahele and A. L. Cullen, "Electric probe measurement on microstrip," *IEEE Trans. Microwave Theory Tech.*, vol. MTT-28, pp. 752–755, July. 1980.

[5] Y. J. Gao and I. Wolff, "A simple electric near field probe for microwave circuit diagnostics," in *IEEE MTT-S Int. Microwave Symp. Digest*, vol. 3, San Francisco, CA, June 18–20, 1996, pp. 1537–1540.

[6] S. S. Osofsky and S. E. Schwarz, "Design and performance of a non-conducting probe for measurements on high-frequency planar circuits," *IEEE Trans. Microwave Theory Tech.*, vol. 40, pp. 1701–1708, Aug. 1992.

[7] Y. J. Gao and I. Wolff, "A new miniature magnetic field probe for measuring three-dimensional fields in planar high-frequency circuits," *IEEE Trans. Microwave Theory Tech.*, vol. 44, pp. 911–918, June 1996.

[8] K. S. Yee, "Numerical solution of initial boundary value problems involving Maxwell's equations in isotropic media," *IEEE Trans. Antennas Propagat.*, vol. AP-14, pp. 302–307, Mar. 1966.

[9] X. Zhang and K. K. Mei, "Time-domain finite difference approach to the calculation of the frequency-dependent characteristics of microstrip discontinuities," *IEEE Trans. Microwave Theory Tech.*, vol. MTT-36, pp. 1775–1787, Dec. 1988.

[10] J. P. Berenger, "A perfectly matched layer for the absorption of Electromagnetic Waves," *J. Comput. Phys.*, vol. 114, pp. 185–200, 1994.

[11] D. S. Katz, E. T. Thiele, and A. Taflove, "Validation and extension to three dimensions of the Berenger PML absorbing boundary condition for FDTD meshes," *IEEE Microwave Guided Wave Lett.*, vol. 4, pp. 268–270, Aug. 1994.

[12] S. Criel, K. Haelvoet L. Martens, D. De Zutter, A. Franchois, R. De Smedt, and P. De Langhe, "Theoretical and experimental quantitative characterization of the near-fields of printed circuit board interconnection structures," in *Proc. IEEE Electromag. Compatibility Symp.*, 1995, pp. 471–474.

[13] R. W. Jackson, "Mode conversion at discontinuities in finite-width conductor-backed coplanar waveguide," *IEEE Trans. Microwave Theory Tech.*, vol. 37, pp. 1582–1589, Oct. 1989.

[14] M. Riaziat, I. Zubeck, S. Band, and G. Zdasiuk, "Coplanar waveguides used in 2–18 GHz distributed amplifier," in *IEEE MTT-S Int. Microwave Symp. Dig.*, June 1986, pp. 337–338.

[15] H. Shigesawa, M. Tsuji, and A. A. Oliner, "Conductor-backed slot line and coplanar waveguide: Dangers and full-wave analyses," in *IEEE MTT-S Int. Microwave Symp. Dig.*, New York, NY, May 1988, pp. 199–202.

[16] N. H. L. Koster, S. Koßlowski, R. Bertenburg, S. Heine, and I. Wolff, "Investigation on air-bridges used for MMIC's in CPW technique," in *Proc. 19th European Microwave Conf.*, London, U.K., Sept. 1989, pp. 666–671.

[17] M. Rittweger, N. H. L. Koster, S. Koßlowski, R. Bertenburg, S. Heine, and I. Wolff, "Full-wave analysis of a modified coplanar air-bridge T-junction," in *Proc. 21th European Microwave Conf.*, Stuttgart, Germany, 1989, pp. 993–998.

[18] V. Radisiæ, D. R. Hjelme, Z. P. Popoviæ, and A. R. Mickelson, "Experimentally verifiable modeling of coplanar waveguide discontinuities," *IEEE Trans. Microwave Theory Tech.*, vol. 41, pp. 1524–1533, Sept. 1993.

[19] G. David, "High frequency characterization of monolithic integrated microwave components and circuits by two-dimensional electrooptic field measurements," Ph.D. dissertation, Univ. Duisburg, Duisburg, Germany, 1996.

[20] C. C. Tien, C. K. C. Tzuang, S. T. Peng, and C. C. Chang, "Transmission characteristics of finite-width conductor-backed coplanar waveguide," *IEEE Trans. Microwave Theory Tech.*, vol. 41, pp. 1616–1642, Sept. 1993.

Yingjie Gao was born in Harbin, China, in 1962. He received the B.Sc. degree in electrical engineering from the Harbin Electronic College, Harbin, China, in 1984, the M.Sc. degree in electrical engineering from the Technical University Harbin, Harbin, China, in 1987, and the Ph.D. degree in electrical engineering from Gerhard Mecator University Duisburg, Duisburg, Germany, in 1997.

Since 1994, he has been a Research Scientist at the Institute of Mobile and Satellite Communication Techniques (IMST), Kamp-Lintfort, Germany. His main area of research is electromagnetic compatibility (EMC).

Andreas Lauer was born in Duisburg, Germany, on December, 15th 1966. He received the Diploma-Degree from Duisburg University, Duisburg, Germany, in 1992.

He is currently with the Microwave Circuits Department, Institute of Mobile and Satellite Communication Techniques, Kamp-Lintfort, Germany. His research interests include electromagnetic simulations (FDTD, method of moments (MOM), etc.), microwave propagation, antennas, waveguides, electromagnetic theory.

Qiming Ren was born in Tianjin, China, on July 18, 1963. He received the B.Sc. and M.Sc. degrees in electronics from Northwest Telecommunications Engineering Institute (now Xidian University), Xi'an, China, in 1985 and 1988, respectively, and is currently working toward the Ph.D. degree at Gerhard Mercator University Duisburg, Germany.

From 1988 to 1994, he was with Nanjing Electronic Devices Institute, Nanjing, China, where he worked in the area of MMIC's, internal matched MESFET power transistors, and nonlinear circuit computer-aided design (CAD) techniques. His research interests are linearization techniques for mobile communication transmitters, microwave circuits, and nonlinear theory

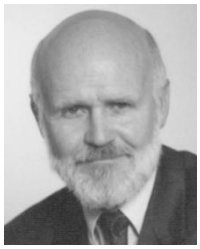

Ingo Wolff (M'75–SM'85–F'88) was born in Köslin, Germany, in 1938. He received the Dipl.-Ing. degree in electrical engineering, the doctoral degree, and the habilitation degree from the Technical University of Aachen, Aachen, Germany, in 1964, 1967, and 1970, respectively.

From 1970 to 1974, he was a Lecturer and Associate Professor for high-frequency techniques at the University of Aachen. Since 1974, he has been a Full Professor of electromagnetic field theory at the University of Duisburg, Duisburg, Germany. His main areas of research are electromagnetic-field theory applied to the CAD of MIC's and MMIC's, millimeter-wave components and circuits, and the field theory of anisotropic materials. Since 1992, he is (parallel to his university position) the Managing Director of the Institute of Mobile and Satellite Communication Techniques (IMST), Kamp-Lintfort, Germany, which is a research and development institute specializing in the areas of mobile communication techniques, microwave and millimeter-wave communication techniques, antenna techniques, and electromagnetic compatibility and environment.